Pellet cloud distribution and dynamics for different plasma scenarios in ASDEX Upgrade and JET

G. Kocsis[1], J.A. Alonso[2], B. Alper[6], G. Arnoux[6], G. Cseh[1], J. Figueiredo[3], D. Frigione[4], L.Garzotti[6], J. Hobirk[5], S. Kálvin[1], M. Lampert[1], P.T. Lang[5], G. Petravich[1], T. Szepesi[1], R. Wenninger[5], ASDEX Upgrade Team and JET-EFDA contributors[*]

JET-EFDA, Culham Science Centre, OX14 3DB, Abingdon, OXON, UK

[1]*KFKI RMKI, EURATOM Association, P.O.Box 49, H-1525 Budapest-114, Hungary,*

[2]*Laboratorio Nacional de Fusion, Euratom-CIEMAT, 28040 Madrid, Spain,*

[3]*Association EURATOM–IST, Av. Rovisco Pais, 1049-001 Lisbon, Portugal,*

[4]*Associazione EURATOM-ENEA sulla Fusione, CP 65, Frascati, Rome, Italy,*

[5]*MPI für Plasmaphysik, EURATOM Assoc., Boltzmannstr. 2, 85748 Garching, Germany,*

[6]*Euratom/UKAEA Fusion Association, Culham Science Centre, Abingdon, OX14 3DB, UK*

[*]See the Appendix of F.Romanelli et al., Fusion Energy (Proc. 22nd Int. Conf. Chengdu) IAEA, 2008

Pellet ELM pacemaking is one of the recently proposed methods to mitigate the ELM caused heat load on plasma facing components of an ITER class tokamak. The increase of the ELM frequency by frequent injection of shallow penetrating cryogenic pellets seems to be a working technique which was demonstrated on ASDEX Upgrade [1] and JET [2]. To optimize this tool the understanding of the underlying physical processes of the pellet ELM triggering is inevitable. The basic question to be answered is the nature and the location of the seed perturbation [4] - introduced by the ablating pellet - which is indispensable for triggering a type-I ELM. To answer this question the interaction of cryogenic pellets with hot plasma has to be understand in details.

To study this interaction (pellet caused perturbations, ELM triggering and pellet cloud dynamics) fast visible imaging by using different fast framing cameras (CCD and CMOS) was recently developed and installed both at ASDEX Upgrade and JET. The pellet-plasma interaction was investigated on both machines in different scenarios to exploit the fast camera diagnostics, results are presented in the following.

Figure 1: *ASDEX Upgrade experimental set-up: cameras detect the pellet cloud radiation from radial ('radial view'), toroidal ('tangential view') and vertical ('top view') directions.*

ASDEX Upgrade

On ASDEX Upgrade tokamak the fast framing pellet observation system [3] consists of several PCO cameras observing the pellet cloud radiation from different directions (radial, toroidal, vertical) with good spatio-temporal resolution (see Fig. 1). Investigations are recently concentrated on the measurement of cryogenic pellet cloud distribution and dynamics. Pellets were injected into OH and H-mode plasmas from the HFS of the tokamak. A database is built containing short exposure pellet cloud images (up to a few μs) recorded in the visible spectral range by radial viewing cameras (Fig. 1), pellet and local plasma parameters. Line cuts along the designated pellet trajectory and magnetic field lines crossing the cloud and their moments and the other scalar parameters (e.g. FWHM) are also calculated and inserted into the database.
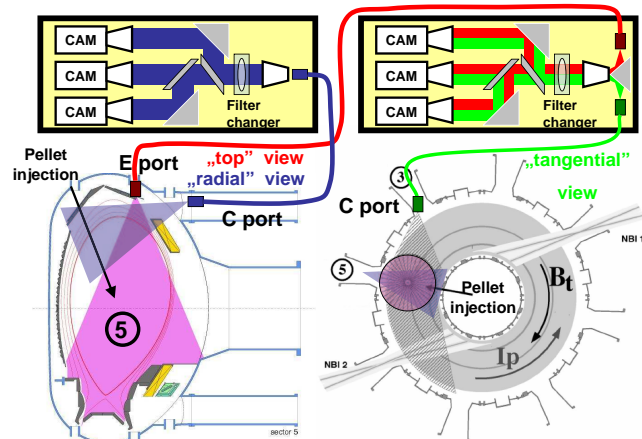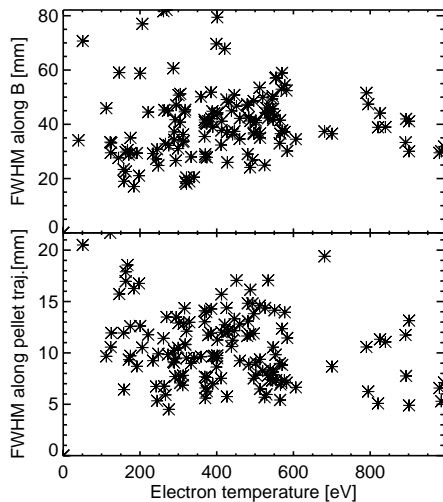
Figure 2: *The FWHM of the clouds in the database along the magnetic field line crossing the cloud (upper part) and along the designated pellet trajectory (lower part).*

To exploit the database first the cloud elongation along magnetic field lines and the diameter in the perpendicular direction are plotted as a function of the local plasma temperature (Fig. 2). It can be observed that the typical FWHM of cloud is about 40mm and 10mm parallel and perpendicular to the magnetic field, respectively. These data show a large variation but no obvious electron temperature dependence. However, it has to be emphasized that the cloud distribution depends not only on the local plasma parameters (dominantly temperature) but probably also on the actual pellet size which is not yet deconvoluted.

Using the database typical cloud patterns are mapped revealing a complex structure (see lower part of Fig. 3). The pellet cloud is elongated along the magnetic field line and has one or two local maxima (hollow distribution). On the images single and double stripes can be observed as well. The delay of the exposure of each camera can be set independently which allows us to investigate the evolution of the pellet cloud radiation parallel and perpendicular to the magnetic field. An example is seen on Fig. 3 where three cameras where triggered by $0,2,4\mu s$ delay. The upper part of this figure shows line cuts (along the designated pellet trajectory) of multiple exposure images [3] of these cameras and the lower part the according

images about the cloud No.1. It can be seen that the pellet cloud shape changes very fast within a few μs. Longer delay times are also used (10,20 μs) to reveal whether the cloud moves together with the pellet (with the pellet velocity) or the pellet fuels consecutive flux tubes. Results are ambiguous because it seems both cases can be observed. We thus conclude the pellet cloud moves with the pellet for some time in the order of $10\mu s$ before its cross-field motion is stopped.

The pellet cloud drift was also investigated by using images of tangential view. It was observed that time to time the pellet cloud detaches from the pellet showing an upward and radial movement with a velocity of 5-10km/s. The radial motion of the cloud is probably caused by the grad(B) drift but the origin of the upward motion is not yet understood.

JET

On JET a Photron APX camera has been recently installed on the 'visible branch' of
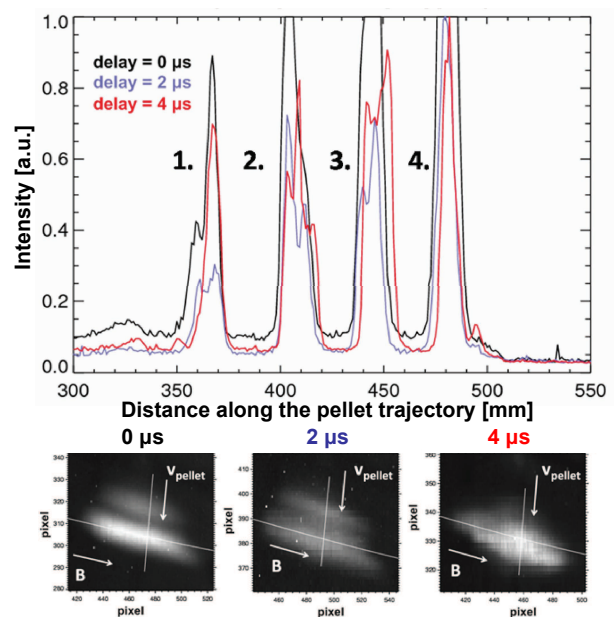

Figure 3: *Line-cut - along the designated pellet trajectory - of multiple exposure images made with different delay times (upper part) and images with different delay time about the cloud No. 1.*

the infrared endoscope. The view involves the full poloidal cross section of the vacuum vessel covering a toroidal extent of 90 degrees (Fig. 4). The cross section of the pellet injection path is in the center of the view making it especially useful to investigate pellet ablation on the $10\mu s$ timescale. Pellets injected from the LFS are the subject of our investigations. An angle of

about 30 degrees between line of sight and pellet track causes difficulties for the pellet tracking but yields a good opportunity to investigate field aligned structures. Fast framing movies recorded during pellet ablation in L-mode and H-mode discharges were analyzed.
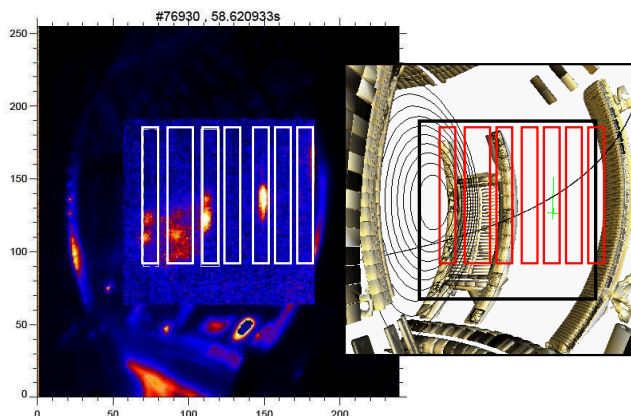

Figure 4: *The view of the fast visible imaging on JET. Left a slow framing image showing the whole cross section is over-plotted with a fast framing one. On right the computer model of the view together with equilibrium magnetic surfaces of the poloidal plane of the pellet injection and a field line started where the pellet crossed the separatrix. The white (red on right) boxes are used during the image processing.*

Because of the relatively low plasma temperature in L-mode discharges pellets with the velocity of about 100-200m/s penetrate deep into the plasma causing clear cooling of the according region. Pellet cloud detachment could be observed on the movies. Time to time the cloud moved vertically and/or horizontally (to LFS) from the pellet. Sometimes extreme long living ($\sim 100\mu s$) horizontally drifting clouds passing long distances could be tracked. Due to the injection and viewing geometry such a long drift track obviously cannot be explained by the LFS drift alone, we assume a toroidal cloud movement takes place as well.

Pellet injected into type-I ELMy H-mode plasmas triggers an ELM shortly after the onset of the ablation. The ELM can be identified on every Mirnov coil signals (located either on the HFS or LFS) as large amplitude high frequency fluctuation. These signals are used to determine the 'MHD onset' of the ELM: the envelope of this fluctuation is calculated and the onset time was defined when it exceeds a predefined threshold. This onset was computed for several coil signals and the earliest one was selected as the 'MHD ELM onset' time (Fig. 5).

On fast framing images (e.g. 70kframe/s) the ablating pellet appears as a bright spot in box 2 (see Fig. 5). At the MHD ELM onset a field line elongated structure - evolving out of the pellet cloud - is formed: bright spots become visible on limiter elements (see box 1,3,5). To visualize the location and movement of these bright spots the radiation within a box - defined around the limiter - was integrated along the horizontal axis (within the box) obtaining the box radiation along the vertical axis. This distribution was calculated for each frames and boxes and was plotted as a function of time. The time axis is created by retrieving the frame times which were measured at high resolution. The typical inaccuracy was in the order of the separation of consecutive frames. The time evolution of the radiation distribution of the above defined seven boxes are plotted in Fig. 6 for a triggered ELM (left) and for a natural ELM (right). Analyzing several ELM events the following typical patterns can be observed. For the pellet triggered case a field line elongated filament is growing out from the pellet cloud. At the same time bright spots on limiter elements appear - indicating for the interaction of this filament with the plasma facing components. The appearance of this field aligned structure coincides with the MHD ELM onset. After detachment from the pellet cloud this structure rotates toroidally or poloidally (the bright spots on limiter elements move upward) until it is slowed down after about $100\mu s$. For natural type-I ELMs such helical structures could also be observed as bright spots on limiter elements. However, the onset of this high activity plasma-wall interaction does not always coincide with the MHD onset of the ELMs but varied between 0 and $100\mu s$ after it.
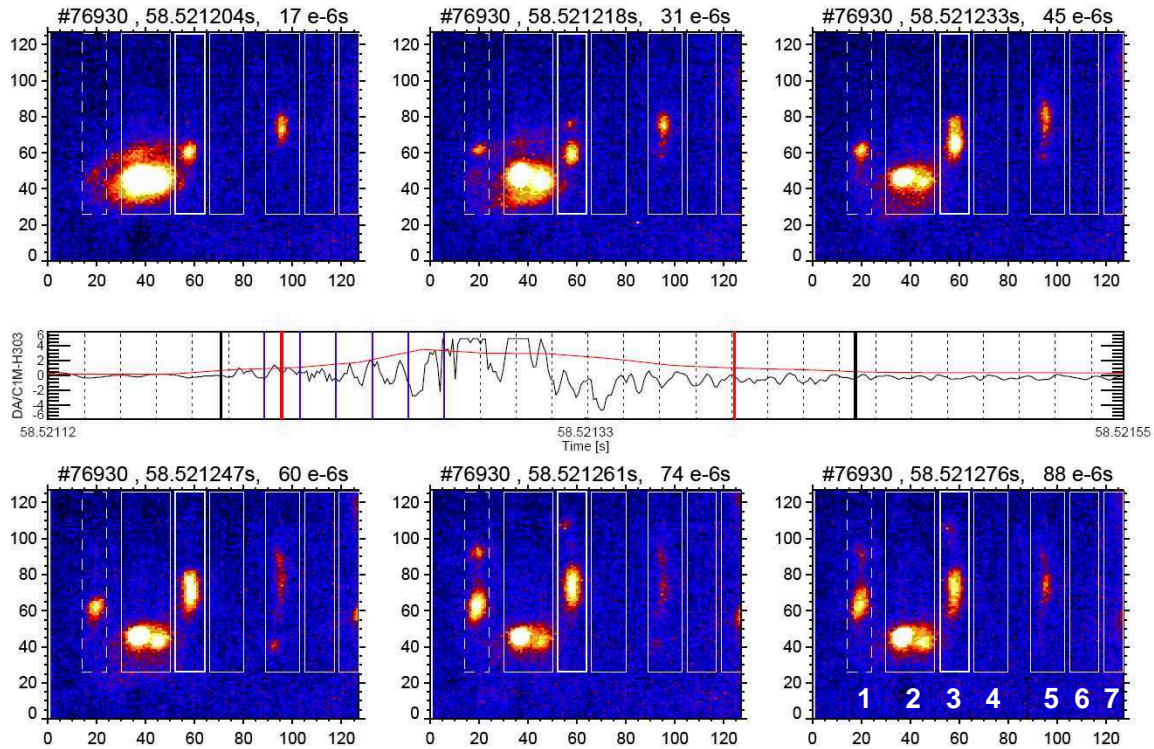
Figure 5: *Mirnov coil signal (middle) during a pellet triggered ELM with its high frequency envelope (red) and the calculated ELM onset time (over-plotted red vertical line). The black vertical line denotes the ELM MHD onset. The six plots around are successive frames of the fast camera, their frame times are marked on the Mirnov coil signal by blue vertical lines. The white boxes are used for image processing encircling the left ILA limiter (1), the pellet ablation location (2), the right ILA limiter (3), inter limiter areas (4,6) and middle of the antenna (5) which acts as limiter and the edge of the last limiter seen on the images (7).*

From these observations it may be concluded that for LFS pellet injection a filament evolves directly out of the cold, high pressure pellet cloud which could be the seed perturbation which in turn evolutes into an ELM. Natural ELMs are born at an arbitrary toroidal location and it takes some time before the perturbation becomes detectable in the observation volume of the visible imaging. This assumption will be investigated and further refined by analyzing the pellet ELM triggering for HFS pellet injection which is the subject of our future investigations.
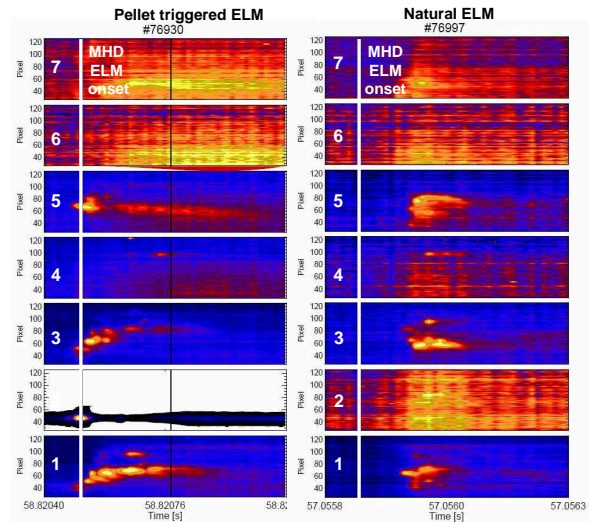

Figure 6: *The time evolution of the distribution of box radiation for the above defined seven boxes for a triggered ELM (left) and for a natural ELM (right). The MHD ELM onset is also over-plotted (white vertical line).*

References

[1] P.T. Lang et al., NF, **43**, 1110 (2003)

[2] P.T. Lang et al., this conference, P4.163

[3] G. Kocsis et al., RSI, **75**, 4754 (2004)

[4] G. Kocsis et al., NF, **47**, 1166 (2007)